Journal of the Serbian Chemical Society
JSCS-info@shd.org.rs • www.shd.org.rs/JSCS
J. Serb. Chem. Soc. *83* (2) 181–198 (2018)
JSCS–5067
UDC 549.514.62+544.6.076.32:544.52:667.28:621.383.51:532.135
Original scientific paper

The synthesis of transparent TiO_2 photoelectrodes assisted by rheological agents Triton X-100, PVP and F-127 for dye sensitized solar cells

JOAN REYES MIRANDA[1,2], ÁNGEL DE JESÚS MORALES RAMÍREZ[1]*, FELIPE DE JESÚS CARRILLO ROMO[1], ANTONIETA GARCÍA MURILLO[1], ELDER DE LA ROSA CRUZ[3], CÉSAR A. FLORES SANDOVAL[4], ARISTEO GARRIDO HERNÁNDEZ[5] and DULCE YOLOTZIN MEDINA VELÁZQUEZ[2]

[1]Instituto Politécnico Nacional, CIITEC IPN, Cerrada de Cecati S/N. Col. Santa Catarina, Azcapotzalco México D.F. C.P 02250, México, [2]Universidad Autónoma Metropolitana UAM-Azcapotzalco, San Pablo Xalpa No 180. Col Reynosa Tamaulipas, Azcapotzalco, México D.F. C.P. 08100, [3]Centro de Investigaciones en Óptica A.C, A.P. 1-94837150, León, Gto., México, [4]Instituto Mexicano del Petróleo, Programa de Ingeniería Molecular, Eje Central Lázaro Cárdenas No. 152, San Bartolo Atepehuacan, C.P. 07730, Distrito Federal, México and [5]Universidad Tecnológica de Tecámac, División de Nanotecnología, Carretera Federal México-Pachuca Km 37.5, Sierra Hermosa, 55740, Edo. De México, México

(Received 15 March, revised 25 April, accepted 28 April 2017)

Abstract: In this work, the transparent TiO_2 photoelectrodes have been synthesized by the sol–gel method and the dip-coating technique, incorporating three rheological agents as porous template – Triton X-100, polivinilpirrolidone (M.W. 10000) and Pluronic F-127 into the TiO_2 sol for the application in dye-sensitized solar cells. Fourier transform infrared spectroscopy, X-ray diffraction, scanning electron microscopy, m-lines and UV–Vis spectroscopy analyses were carried out to examine the chemical composition, structure, morphology, thickness and optical transmittance of the TiO_2 photoelectrodes. Impedance spectroscopy was carried out to analyze the cells' behaviour. An average energy conversion efficiency of 1.04 % was achieved using triton as a modifier of the transparent TiO_2 film, obtaining a thickness about 1.21 μm, a crystallite size of about 7 nm in the anatase phase and the porosity of about 53.4 %. Triton proved to be efficient for obtaining transparent and porous semiconductor films, while increasing the photoelectrochemical device's performance.

Keywords: transparent films; photoelectrodes; sol-gel; anatase

* Corresponding author. E-mail: angel_ipn77@hotmail.com
https://doi.org/10.2298/JSC170315058R

INTRODUCTION

Energy plays an essential role in the human social and economic life. The functioning of society depends completely on its availability and administration. Energy mainly comes from fossil fuels, which cover approximately 80% of the world energy requirements: near 36 % corresponding to oil, 24 % to coal, and 20 % to natural gas.[1] However, the effects on climate change of the production and consumption energy from fossil fuels impose an urgent need for the adjustments in the way the energy is generated and consumed. There is a clear need to reduce the use of fossil fuels and greenhouse gases emissions, *i.e.*, sustainable energy should be a priority energy option in order to satisfy current demand without compromising the needs of future generations.

Solar energy is the most abundant resource on the earth; however, the electric power obtained using solar cells provides only 0.1% of total energy generation,[2] mainly from traditional silicon solar cells. The main problem with the solar cells is the high purity of silicon required (~99.99%), which makes them expensive. Dye-sensitized solar cells (DSSC), based on metal oxide semiconductor materials, have attracted a great deal of interest, due to their low cost, easy fabrication and relatively high energy conversion.[3] DSSCs consist of a dye-sensitized nanocrystalline semiconductor film, a liquid electrolyte containing an I^-/I_3^- redox couple, and a platinized transparent conducting oxide as a counter-electrode. As the matrix of these systems, the TiO_2 semiconductor receives a great deal of attention due to its advantages, such as its low cost, environmental compatibility and corrosion resistance.[4–6] The photovoltaic properties of DSSC are mainly influenced by the quality of the TiO_2 film, *i.e.*, its crystalline structure, crystallite size, surface area, porosity, thickness and so forth.[7] Porous TiO_2 photoelectrodes are the components most critical for achieving the light harvesting from the dye and the electron injection into the TiO_2, whereas smooth ones adsorb few dye molecules and have poor cell performance. The preparation method of the TiO_2 films has a great effect on these properties; several deposition methods, such as sputtering, chemical vapour deposition, spin coating, and sol–gel, are used to obtain TiO_2 films.[8–14] Among these methods, the sol–gel has considerable advantages, such as a low processing temperature, the capacity to obtain nanostructures, chemical homogeneity, controlled and homogeneous doping.[15–18] However, the main limitation of the sol–gel method is the low thickness obtained by dip-coating deposition; therefore, the dissolution of rheological agents (RA) in the sol, *i.e.*, Triton, PVP, Pluronic F-127, Brij, *etc.*, is a promising approach for the increase of its viscosity and thereby obtaining a thicker TiO_2 film, without losing its transparency. Moreover, the rheological agents are considered porous templates; when they are dissolved in the sol, they begin to segregate and form micelles, after which the alkoxide precursors undergo hydrolysis

and condensation reactions around the micelles; finally, an annealing treatment removes the organic compounds and promotes porosity in the material.[19]

TiO_2 films have been synthesized by the sol–gel method using rheological agents. B. Guo *et al.*[20] synthesized porous films using PEG with different molecular weights 200, 600, 1000 and 6000 as porous templates, and the TiO_2 films were obtained using the spin-coating technique. Along with an increase in molecular weight, the porous size increased and the crystallite size decreased, and a surface area of 7.5 $m^2 g^{-1}$ without adding PEG as well as 19.24 $m^2 g^{-1}$ using PEG 6000 was reported. Urh Cernigoj *et al.*[21] synthesized TiO_2 films using Brig 56, Triton X-100 and Pluronic F-127. Transparent and free-crack TiO_2 films were obtained, and rheological agents retarded the films' crystallization, producing smaller crystallite sizes of ~10 and 11 nm using Pluronic and Brig, respectively, while without surfactants, the crystallite size was about 18 nm. E. C. Muniz *et al.*[22] produced mesoporous TiO_2 films using Triton X-100 as a porous template. A large surface area of about 80 $m^2 g^{-1}$ and a crystallite size about 15–20 nm, attributed to the use of Triton X-100, were reported. H. Segawa *et al.*[23] studied the effect of PVP (molecular weight: 10000, 40000 and 360000) on the synthesis of TiO_2 films; they found that when the molecular weight increased, the sol viscosity increased as well. Crack-free TiO_2 films were produced with PVP 40000 and with a thickness of 400 nm for each coating; with PVP 3600, cracks were observed. S. J. Darzi *et al.*[24] prepared TiO_2 films using Pluronic P-123 as a porous template and reported a crystallite size of about 7.4 nm and a surface area of about 124.3 $m^2 g^{-1}$. S. R. Patil *et al.*[25] obtained TiO_2 films using Pluronic F-127 as a porous template. The crystallite sizes reported were around 24 nm and 11 nm without surfactants and in the presence of F-127; the surface area was about 48 $m^2 g^{-1}$ and 127 $m^2 g^{-1}$, with and without surfactants, respectively. However, the effects of rheological agents on the synthesis of TiO_2 photoelectrodes and their photoelectrical properties, when assembled in dye-sensitized solar cells, have not yet been reported. Considering this, the aim of this work is to study the effects of Triton, PVP and F-127, testing their photovoltaic properties as a function of crystallite size, crystalline structure, thickness and porosity of the TiO_2 films obtained.

EXPERIMENTAL

Materials

The precursor material for TiO_2 sol synthesis was titanium butoxide ($Ti(O(CH_2)_3CH_3)_4$; 97 %, Fluka). Hydrolysis and condensation reactions were carried out with acetic acid glacial (CH_3COOH, Sigma-Aldrich), isopropanol (C_3H_8O; 99.8 %, Sigma–Aldrich), methanol anhydrous (CH_4O, 99.8 %, Sigma–Aldrich) and the rheological agents Triton X-100 ($(C_2H_4O)_nC_{14}H_{22}O$), polyvinylpyrrolidone ($(C_6H_9NO)_n$) and Pluronic F-127, which were purchased from Sigma–Aldrich. Indium-doped SnO_2 (ITO-Aldrich), with a surface resistivity of about 30-60 Ω-m^{-2}, and SiO_2 slides were used as substrates for the TiO_2 films and the N-719

dye (di-tetrabutylammonium cis-bis(isothiocyanato)bis(2,2'-bipyridyl-4,4'-dicarboxylato) ruthenium-(II), Sigma-Aldrich) was used for sensitizing the TiO_2 films.

Synthesis of TiO_2 in presence of rheological agents

In a typical synthesis, 6.46 mmol of titanium butoxide precursor was modified with 38.78 mmol of acetic acid under vigorous magnetic stirring for 10 min, producing an exothermic reaction and a transparent solution. Afterwards, 13 mmol of isopropanol was added to the solution, maintaining the solution under agitation for 10 min. Later, a 174.54 mmol solution of methanol was incorporated, and the resulting solution was kept stirring for 30 min. The solvents mole ratios in respect to titanium butoxide were $1Ti(O(CH_2)_3CH_3)_4$: $:6CH_3COOH:2C_3H_8O:27CH_4O$. Acetic acid was used, due to the difficulty of forming stable salts using precursors with a high reactivity with water (titanium alkoxides); the alternative is to form non-aqueous solutions that make it possible to obtain TiO_2 sols with stable precursor solutions and less reactivity.[26,27] Acetic acid modified the precursor to form a titanium acetate precursor that was stable and less reactive.[28]

Finally, the rheological agents were incorporated into the TiO_2 sol, and the solution was stirred continuously for 60 min. Five different systems were prepared with different concentrations of the rheological agents. The mole ratios of the rheological agents regarding Ti were: 1Ti:*x*Triton (*x* = 0.25, 0.50, 0.75, 1, 1.25), 1Ti:*y*PVP (*y* = 0.1, 0.2, 0.3, 0.4, 0.5) and 1Ti:*z*Pluronic F-127 (*z* = 0.025, 0.05, 0.075, 0.1, 0.125). The concentration of each rheological agent was determined by the optical quality of the films; *i.e.*, transparency, homogeneity and crack free surfaces. Rheological agents increase the sol viscosity, enabling a greater thickness for each deposited layer to be obtained; porosity is increased and the dye impregnation enhances the absorption of light.

Film deposition and preparation of the solar cells

The TiO_2 films were deposited on both glass and indium tin oxide (ITO) substrates by the dip-coating technique. The rate used was 0.36 cm s^{-1}. Before the deposition of the films, the substrates were perfectly cleaned in an ultrasound bath; first in distilled water with soap for 10 min, then in hot distilled water for 10 min, and finally, in methanol for 10 min. Once the first TiO_2 layer was formed, the films were dried for 10 min at 100 °C to obtain a xerogel;

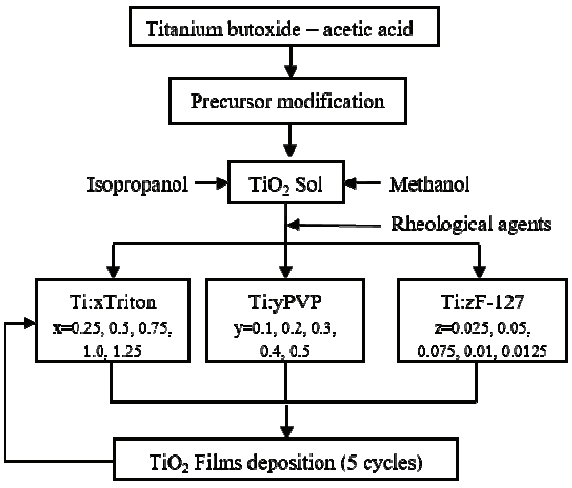

Scheme 1. Synthesis procedure for the TiO_2 films.

then an annealing treatment was carried out at 300 °C for 10 min, and finally at 500 °C for 10 min to induce crystallization of the films. Scheme 1 shows the synthetic procedure. The temperature ramp (100, 300 and 500 °C) was chosen to avoid crack formation. The cycle was repeated five times to increase the film thickness. Finally, the films were annealed at 500° C for 60 min.

The prepared TiO_2 films coated onto ITO substrates were sensitized with N-719 dye. A 0.3 mM solution of N-719 dye in ethanol was prepared and kept stirring for 30 min. Before sensitization, the films were dried at 80 °C for 1 h and then dipped into the dye solution for 24 h at room temperature. The sensitization was carried out inside a desiccator to avoid hydration of the TiO_2 photoelectrodes and to enhance the dye adsorption. Finally, the photoelectrodes were washed with ethanol to remove the excess adsorbed dye on the TiO_2 surface. The photoelectrodes were assembled with a Pt counter-electrode and I^-/I_3^- electrolyte to form a sandwich-type cell.

Characterization and measurements

The IR spectra were recorded using a Perkin Elmer 2000 FTIR Waltham, MA, the results obtained were in the 4000–400 cm^{-1} range using the KBr pellet technique. The crystalline structure of the TiO_2 films was obtained using a powder diffractometer (Siemens D5000) with CuKα radiaton (λ = 1.54056 Å), operated at 35 kV, 25 mA. A step of 0.15°s^{-1} was used in the 20–80° range. The morphology of the samples was examined using a scanning electron microscope (JEOL JSM-6390LV). The thickness and porosity of the samples were measured using m-lines spectroscopy, employing a He–Ne laser with λ = 632.8 nm. The transmittance spectra were recorded by using a Spectrometer Perkin Elmer, model Lambda 35 UV–Vis. The photocurrent–voltage (J–V) curves were obtained using an Oriel^R Sol3A^{TM} Class AAA solar simulator with a 450 W Xe lamp (Newport 6279NS) and an Air Mass 1.5 G filter for spectral correction to illuminate the sensitized solar cell.

RESULTS AND DISCUSSION

Chemical analyses by FTIR spectroscopy

The bond evolution of synthesized ceramics was studied using FTIR spectroscopy on the TiO_2 xerogel dried at 100 °C. Fig. 1 shows the bond evolution of TiO_2 from the xerogel stage (100 °C) up to the formation of the Ti-O bonds (500 °C). These spectra show stretching bands corresponding to hydroxyl groups ν(OH)[29,30] in the range from 3600 to 3000 cm^{-1}, which came from the molecular water and the water adsorbed on powders, due to moisture in the environment. The centered band at 1718 cm^{-1} corresponds to the stretching vibrations of C=O, ν(COO)[28] and indicates the presence of free acetic acid; this band appeared at temperatures up to 300 °C. The two centered bands at 1550 and 1440 cm^{-1} are related to asymmetric vibrations, ν_{asym}(COO), and symmetric vibrations, ν_{sym}(COO), respectively. [28] The coordination mode between Ti^{4+} and the acetate ligand CH_3COO^-, in respect to the difference frequency ($\Delta\nu$ = 110 cm^{-1}) of the asymmetric and symmetric vibrations of COO^-, suggests that acetate acted as a chelating acetate ligand, which means Ti^{4+} was bonded to the two oxygen atoms of CH_3COO^-, relating to the modification from titanium butoxide to titanium acetate $Ti(OR)_x(Ac)_y$.[28,30] The hydrolysis of this chelating acetate was slower than

that of the OR groups coming from $Ti(OBu)_4$; therefore, there was an increase in gelation time, favouring polycondensation processes. The intensity of these bands decreased when the temperature increased; however, they did not disappear completely. The band at 1029 cm^{-1} is related to the vibrations of butoxy groups bonded directly to the titanium.[28] These bands were still present at 300 °C, but at 400 °C they disappeared completely. The main characteristic of these spectra at 400 and 500 °C is the intense band centred at 520 cm^{-1}, which corresponds to stretching vibrations ν(Ti–O–Ti) related to the characteristic octahedral TiO_6 of TiO_2.[31] An annealing treatment at 500 °C for 1 hour insured the formation of Ti–O–Ti bonds. However, a longer time or higher temperature in the annealing treatment would promote crystallite growth as well as a possible phase transition, completely eliminating the bands related to the asymmetric and symmetric vibrations of the free acetate groups (COO).

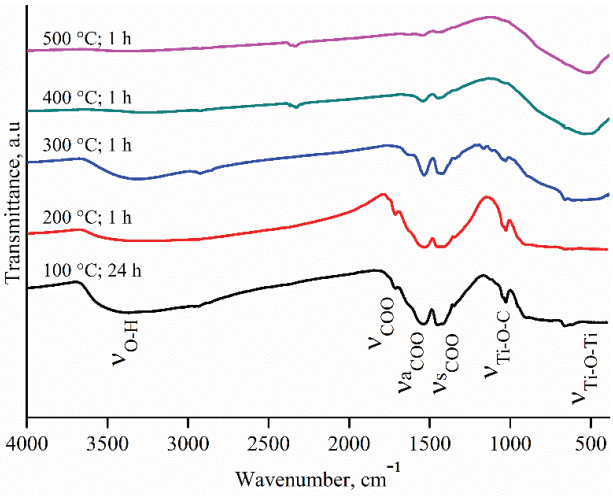

Fig. 1. Infrared spectra of the TiO_2 powders at different annealing temperatures.

Fig. S-1 of the Supplementary material to this paper shows the infrared spectra after the rheological agents were incorporated into the TiO_2 precursor solution. These spectra correspond to the mole ratios of the rheological agents: Ti:Triton = 1:0.5, Ti:PVP = 1:0.2 and Ti:F-127 = 1:0.075. The spectra obtained after an annealing treatment at 500 °C for 60 min showed the characteristic stretching vibration bands of Ti-O-Ti bonds. All of the samples containing rheological agents were analyzed and showed no considerable changes.

X-Ray diffraction

Fig. 2 shows the X-ray diffraction patterns of the TiO_2 films, with and without the RAs. These patterns correspond to the mole ratios of the rheological

agents: Ti:Triton = 1:0.5, Ti:PVP = 1:0.2 and Ti:F-127 = 1:0.075. The patterns show a strong diffraction peak at 2θ = 25.4° corresponding only to the (101) plane indexed to the anatase tetragonal crystalline structure according to JCPDS 71-1166.[32] The sol–gel and dip-coating process produced the formation of a highly oriented anatase phase along the (101) plane; $I_{(101)}/I_T$ = 0.75 with and without the surfactants.[21]

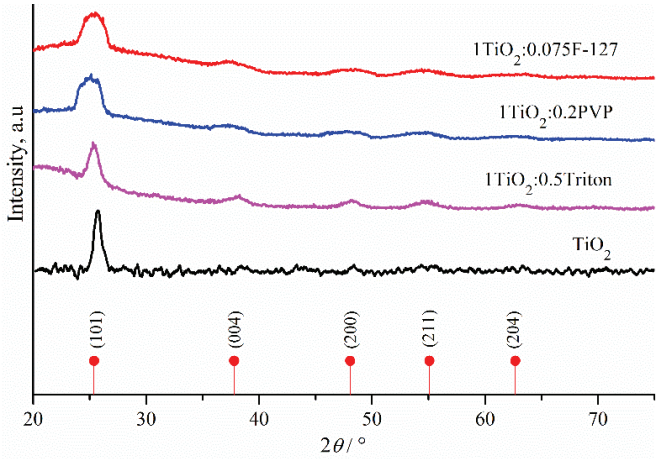

Fig. 2. X-ray diffraction of the TiO_2 films without RAs (a) and in the presence of Triton (b), PVP (c) and F-127 (d) annealed at 500 °C for 60 min and coated on SiO_2.

Moreover, as can be observed, adding surfactants produced a shift that was related to a decrease in crystallite size. The TiO_2 crystallite size was estimated using Scherer´s formula:[33]

$$D_{(101)} = \frac{K\lambda}{\beta \cos\theta} \quad (1)$$

where $D_{(101)}$ is the crystallite size for the (101) plane, K is a constant (0.9), λ is the wavelength of the X-rays (CuKα = 0.15418 nm), β is the full width at half maximum (FWHM), and θ is half of the diffraction angle of the centroid at the peak. Table I shows the crystallite size calculated for all of the samples analyzed. The crystallite size calculated for the TiO_2 film without RAs was about 30-35 nm. Adding surfactants to the TiO_2 sol resulted in a reduction of the crystallite size as the surfactant concentration of each system increased; this was related to a growing slowdown of the TiO_2 particles, due to the fact that the hydrolysis and condensation reaction rates took longer to be completed.[20,21,34,35] Moreover, the increase of the surfactant concentration decreased the crystallinity. These patterns promote an amorphous behaviour. The rheological agents, under the synthesis

conditions of TiO_2 photoelectrodes, made it possible to reduce the crystallite size below 10 nm.

TABLE I. Crystallite size as a function of the concentrations of the rheological agents

System	Mole ratio	Crystallite size, nm
Pure TiO_2	–	~25–30
TiO_2:Triton	1:0.25	~6.5
	1:0.50	~7.3
	1:0.75	~6.4
	1:1	~6.0
	1:1.25	~5.8
TiO_2:PVP	1:0.1	~3.4
	1:0.2	~3.9
	1:0.3	~3.5
	1:0.4	~3.6
	1:0.5	~3.7
TiO_2:Pluronic F-127	1:0.025	~3.9
	1:0.05	~3.7
	1:0.075	~3.9
	1:0.1	~4.0

Morphology of TiO_2 films

Fig. 3a shows a SEM image of the TiO_2 film coated onto SiO_2, at 5000×. As can be seen, the film is free of cracks and the coating is homogeneous, demonstrating that the synthetic method can produce crack-free TiO_2 photoelectrodes. Crack-free films are needed to avoid short circuits between the electrolyte and the ITO surface in the operation of solar cells.[36] Fig. 3b shows an image of the TiO_2 film at 100000×, with quasi-spherical particles constituted by ~30–40 nm crystallites. The image suggests there is a uniform crystallite distribution with good connectivity among the particles. During the synthesis, Ti-O-Ti chains formed due to the hydrolysis and condensation reactions. After the annealing treatment, these chains remained to produce the good distribution and connectivity among the TiO_2 particles,[37] but the high surface energy of the nanoparticles caused them to agglomerate; therefore, a small degree of porosity can be observed, preventing an appropriate concentration of dye from attaching to the TiO_2 film surface.

Fig. 3c shows an image of a TiO_2:Triton film; the image shows a small crystallite size compared to pure TiO_2 films. Fine pores can be observed, due to the hydrolysis and condensation reactions of the Ti precursor that occur around Triton, which acted as a barrier among the formed Ti–O–Ti chains. After the annealing treatment, the Triton molecules decompose, increasing the pore content.[20]

The SEM images of the TiO_2 films in the presence of PVP and F-127 (Fig. 3d, e and f) shows smaller crystallite sizes than in the films without surfactants. The rheological agent PVP promoted small pores of uniform density, while F--127 produced larger pores. It is important to note that the temperature decomposition of Triton extends up to 350° C, while PVP and F-127 decompose up to 200° C; this promoted a greater densification of TiO_2 particles in the presence of PVP and F-127 after the 500 °C thermal annealing. The micrograph of the TiO_2 film with F-127 suggests the smallest crystallite size, compared to the films using Triton and PVP.

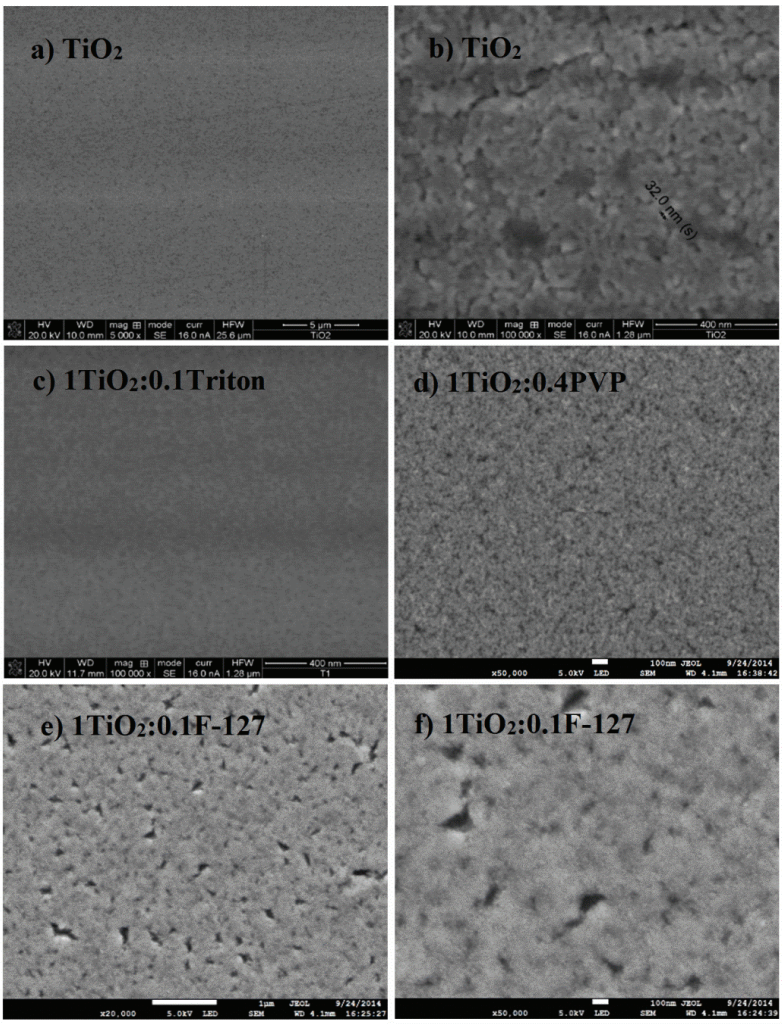

Fig. 3. SEM images of TiO_2 films. a) TiO_2 at 5000×, b) TiO_2 at 100000×, c) TiO_2:Triton at 100000×, d) TiO_2:PVP at 50000×, e) TiO_2:F-127 at 20000× and f) TiO_2:F127 at 50000×.

Optical transmittance

Fig. 4 shows the optical transmittance spectra of the rheological agents assisted TiO_2 films, TiO_2:Triton and TiO_2:PVP. The spectra were recorded in the range of 300 to 700 nm. The first part of the spectra; among 325–375 nm corresponds to the highest light absorption caused by the excitation of electrons from valence band to the conduction band of TiO_2. The second region among 375–700 nm corresponds to transmittance of TiO_2 films. All the samples containing rheological agents showed high transparency in the visible light region (above 80 %), however the pure TiO_2 film showed the poorest transparency (~70 %). High transmittance is related to the small crystallite size which eliminate light scattering.[38] The oscillations in the spectra are due to the interference in the TiO_2 film by the reflections at the air-TiO_2 and TiO_2-substrate interfaces.[39–41]

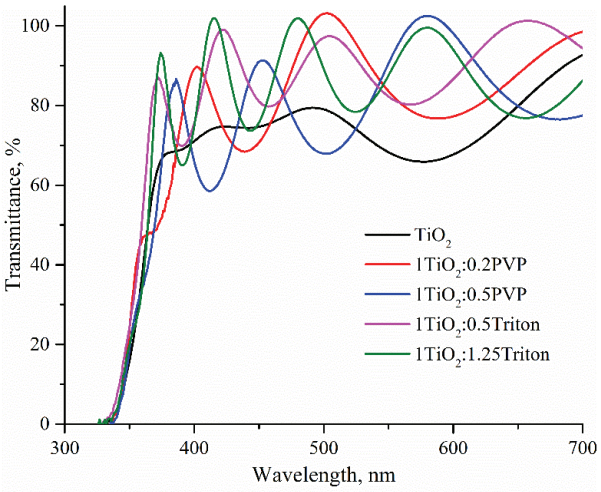

Fig. 4. Transmittance spectra of rheological agents assisted TiO_2 films.

The band gap (E_g) for the films is determined from the optical transmittance spectra by using the Tauc model $(\alpha h\upsilon)^n$ versus photon energy plot:[42–44]

$$(\alpha h\upsilon)^n = B\left(h\upsilon - E_g\right) \tag{2}$$

where α is the absorption coefficient, and is related to transmittance for $\alpha =$ $= -\ln(T/d)$; where d is the film thickness, in our case obtained by m-lines technique, $h\upsilon$ is the photon energy, B is a constant, n is a value that depends on the nature of transition, $n = 2$ to direct and $n = 0.5$, to indirect band gap.[45,46] An indirect band gap for anatase TiO_2 structure has been previously determined.[47] The optical band gap for the pure and assisted rheological TiO_2 films was obtained by extrapolating the linear portion of the $(\alpha h\upsilon)^{0.5}$ *versus* $h\upsilon$ curve to the $h\upsilon$ axis (Fig. S-2 of the Supplementary material). As can be seen, the higher the

rheological concentration, the higher the band gap is. As showed for diffraction patterns and SEM images, as increased the rheological concentration the crystallite size is reduced to 3–10 nm, this is the reason why the obtained band gap is from 3.3–3.5 eV as compared with the bulk band gap of anatase (3.2 eV).[48]

The m-lines study

The TiO_2 films' thickness and refractive indices, with and without RAs, were determined using m-lines spectroscopy by the propagation modes in the films.[49,50] Propagation modes as electromagnetic radiation are transmitted in correspondence with magnetic transverse modes (MT) and electric transverse modes (EM). The analyzed films had at least two electric and two magnetic transverse modes. Table II shows the thickness and refractive indices of the TiO_2 films. As can be seen, the thickness increased as the mole ratio of the rheological agents increased. This phenomenon can be attributed to an increase in the TiO_2 sol viscosity as the concentration of the rheological agents increased, which caused more TiO_2 particles to bond to the substrate during the dip coating process. On the other hand, the refractive index decreased with the increase of the rheological agent's concentration as a consequence of lees crystallinity of the TiO_2, leading to a less dense distribution and less connectivity among the TiO_2 particles.

TABLE II. Opto-geometrical parameters of the TiO_2 films

System	Mole ratio	Thickness, μm	Refractive index
TiO_2	1:0	0.85	2.21
TiO_2:Triton	1:0.25	1.0	2.16
	1:0.50	1.21	1.89
	1:1	3.37	1.84
	1:1.25	3.56	1.84
TiO_2:PVP	1:0.1	1.15	2.18
	1:0.2	1.38	2.03
	1:0.3	1.64	2.05
	1:0.4	2.25	2.02
	1:0.5	2.63	1.99
TiO_2:F-127	1:0.025	1.16	2.02
	1:0.050	1.48	1.98
	1:0.075	1.51	1.98
	1:0.10	1.65	1.96

From the refractive index obtained, it is possible to determine the density and porosity of the TiO_2 films using Lorenz–Lorenz (Eq. (3))[51] and Drude (Eq. (4)) equations:[52]

$$\rho = \frac{K\left(nf^2 - 1\right)}{nf^2 + 2} \tag{3}$$

$$1-P=\frac{\left(nf^2-1\right)}{\left(nb^2-1\right)} \tag{4}$$

where ρ is density, K is a constant obtained from the theoretical density (ρ_t = = 3.9 g cm^{-3}) and the refractive index, nf is the calculated refractive index, nb = = 2.561 is the theoretical refractive index, and P is porosity. Fig. S-3 of the Supplementary material shows graphs of density and porosity as a function of the rheological agents.

Solar cell performance

The photocurrent–photovoltage curve under simulated sunlight 1.5G AM of the cell using a pure TiO_2 photoelectrode is shown in Fig. 5; the overall conversion efficiency (η) was determined by the photocurrent density (J_{sc}), the open-circuit voltage (V_{oc}), the fill factor (FF) of the cell and the intensity of the incident light (Is):[52,53]

$$\eta=J_{sc}V_{oc}\left(\frac{FF}{I_s}\right) \tag{5}$$

The fill factor (FF) was defined as the ratio of the maximum power (P_{max}) obtained from the cell to the theoretical maximum power (P_{th}):

$$FF=\frac{P_{max}}{P_{th}}=\frac{J_{mp}V_{mp}}{J_{sc}V_{oc}} \tag{6}$$

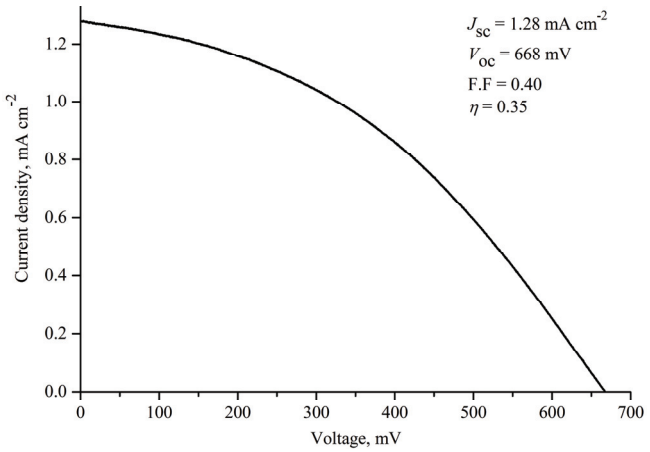

Fig. 5. *J–V* curve of DSSc with the pure TiO_2 photoelectrode.

Under illumination, the N-719 dye molecules anchored on TiO_2 surface absorb the simulated sun light 1.5G AM promoting one electron from the HOMO

to LUMO level of dye, then the electron is transferred to the conduction band of TiO_2 as illustrated in Fig. S-4 of the Supplementary material. The cell generated a long open circuit voltage (V_{oc} = 668 mV), because the N-719 dye produced a high electron injection into the TiO_2 conduction band, resulting in an energy difference between the Fermi level of the injected electrons and the Nernst potential of the redox couple in the electrolyte I^-/I_3^-.[53,54]

However, the short circuit photocurrrent was low (1.28 mA cm^{-2}), promoting the low cell performance, at about 0.35 %. This poor efficiency was mainly related to the low TiO_2 film thickness (~0.85 μm). The second factor affecting the cell efficiency was related to the lack of pores in the TiO_2 film, because only the dye layer was adsorbed on the smooth TiO_2 surface. This parameter produced a non-quadratic curve and a low fill factor (0.4); in addition, the low fill factor was related to the electrons in the conduction band recombining with the electrolyte or the dye. That means that the electrons, instead of being transferred to the counter-electrode, were regenerating the dye molecules or electrolyte, and therefore no current was generated.

Fig. 6 shows the *J–V* curves of the cells fabricated with TiO_2 electrodes containing: Triton, PVP and F-127 with mole ratios of 1:05, 1:0.2 and 1:0.075 respectively. These mole ratios showed the best performance for each rheological agent. In the case of Triton, an enhancement of efficiency was observed, compared to the cells that did not contain a rheological agent. This efficiency enhancement was related to an increase in the TiO_2 film surface area, due to the generation of pores and a reduction of the crystallite size, as well as to an increase in the TiO_2 film thickness, promoting a bigger amount dye adsorption and consequently a greater number of electrons flowing to the counter-electrode, thereby increasing the short-circuit current density (J_{sc}).

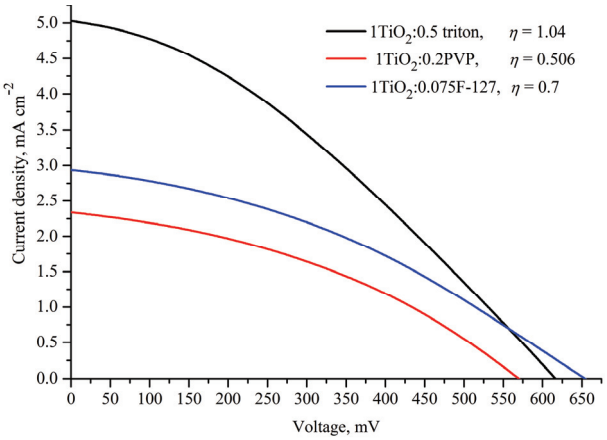

Fig. 6. *J–V* curve of DSSc with the TiO_2 photoelectrode and with the addition of Triton (a), PVP (b) and F-127 (c).

Fig. 7a shows the photovoltaic performance of all of the samples containing Triton in the TiO_2 photoelectrode. It can be seen that maximal efficiency is associated with the system Triton/TiO_2 = 0.5.

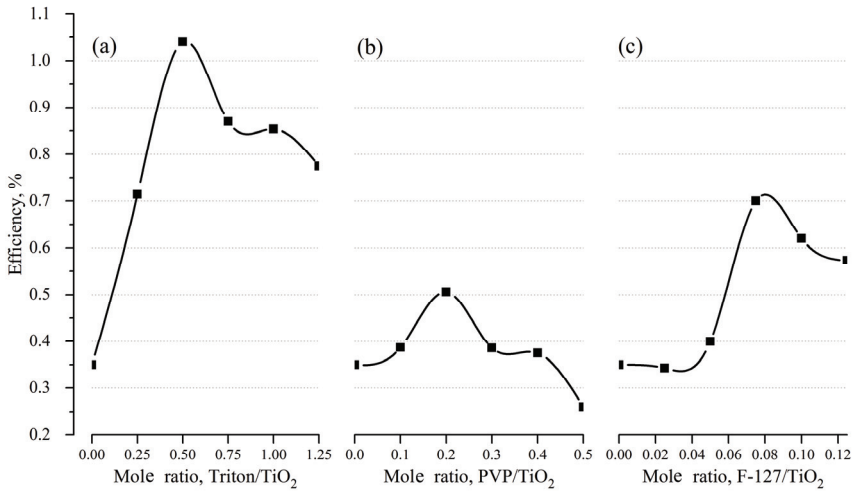

Fig. 7. Conversion efficiency of the cells assembled with TiO_2 photoelectrodes containing rheological agents: a) TiO_2:Triton, b) TiO_2:PVP and c) TiO_2:F-127.

After this concentration, there is a decrease in the photovoltaic performance, which can be attributed to a decrease in TiO_2 crystallinity, as confirmed by XRD, loosening the connectivity among TiO_2 particles, as well as to the increase in the band gap of TiO_2, impeding the electron transport and favouring the recombination processes. The non-quadratic form of the *J–V* curves with the use of Triton is more evident than without the rheological agent in the TiO_2 photoelectrode. Triton produced a decrement in the fill factor (*FF* in 0.34–0.39 range), affecting cell performance due to an increase of recombination processes.

Fig. 7b summarizes the performance of the cells as a function of the PVP concentration added to the TiO_2 sol. The graph shows that there was an increase in performance up to the mole ratio 1TiO_2:0.2PVP. Thereafter, there was a reduction on the cell's performance, in the same manner as with the use of Triton. These phenomena can be attributed to the diminution of crystallinity, the increase in the band gap, as well as to the resulting increase of recombination processes. As the effects of the rheological agents Triton and PVP, F-127 showed an increase in performance at the mole ratio 1TiO_2:0.075F-127; afterwards, a decrement in performance was observed (Fig. 7c).

Table III summarizes all of the photovoltaic parameters obtained with the *J-V* curves of the cells containing RAs. The increased efficiency can be mainly attributed to a decrease of crystallite size, as confirmed by XRD, and the gen-

eration of pores, as shown in SEM images and by m-lines spectroscopy. The increase of thickness negatively affected the solar cell's performance, because the rise of the RA mole ratio increased the thickness of the TiO_2 films; however, there was a diminution of crystallinity and an increase in the band gap of the TiO_2 particles.

TABLE III. Photovoltaic parameters of cells assembled with photoelectrodes containing Triton, PVP and F-127 under sunlight at 100 mW cm^{-2}

System	Cell	Thickness, μm	J_{sc} / mA cm^{-2}	V / mV	FF	η / %
Triton/TiO_2	0.25	1.0	3.24	614	0.36	0.714
	0.5	1.21	5	617	0.34	1.04
	0.75	–	3.3	672	0.39	0.87
	1	3.37	3.4	659	0.38	0.854
	1.25	3.56	3.51	623	0.354	0.775
PVP/TiO_2	0.1	1.15	1.34	691	0.416	0.387
	0.2	1.38	2.33	570	0.38	0.506
	0.3	1.64	1.64	667	0.358	0.386
	0.4	2.25	1.64	616	0.37	0.375
	0.5	2.63	1.12	636	0.364	0.26
F-127/TiO_2	0.025	1.16	1.39	603	0.41	0.343
	0.05	1.48	1.47	637	0.43	0.4
	0.075	1.51	2.94	653.4	0.365	0.7
	0.1	1.65	2.31	703	0.38	0.62
	0.125	–	2.5	691	0.33	0.573

CONCLUSION

Homogeneous, transparent and crack-free TiO_2 films containing RAs were obtained with the following maximal mole ratios: Ti:Triton = 1:1.25, Ti:PVP = = 0.5 and Ti:F-127 = 0.125. For these mole ratios the thicknesses obtained were 3.56, 2.63 and 1.65 μm respectively, according to the results obtained by m-lines spectroscopy.

The films were indexed to the anatase phase without the presence of a rutile phase and the crystallite size was controlled by the presence of the RAs, ranging from 25–30 nm without a RA to 3–8 nm after RA incorporation. However, a decrease in crystallinity in the TiO_2 films was observed as the Triton, PVP and F-127 concentration increased. The band gap of the assisted TiO_2 films was also affected in the rheological concentration; the higher the concentration, the higher the band gap.

The conversion efficiency of the cell using the pure TiO_2 photoelectrode was about 0.35 % and the low performance was attributed to the low thickness and flat TiO_2 film. On the other hand, the maximal dye adsorption on the TiO_2 film resulted from the use of Triton, promoting a conversion efficiency about 1.04 %. Using PVP and F-127, the conversion efficiencies were 0.5 and 0.70 %, respectively.

SUPPLEMENTARY MATERIAL

Additional data and analyses are available electronically at the pages of journal website: http://www.shd.org.rs/JSCS/, or from the corresponding author on request.

Acknowledgements. The authors gratefully acknowledge the financial support of this work by the SEP-CONACYT 136219 project and SIP-IPN projects 20140031, 20140032 and 20140033. The authors also would like to thank Henry Jankiewicz for the editing work that he did for this paper and M. García Murillo for her assistance.

ИЗВОД

СИНТЕЗА ТРАНСПАРЕНТНИХ TiO_2 ФОТОЕЛЕКТРОДА ПОТПОМОГНУТА РЕОЛОШКИМ АГЕНСОМ (TRITON X-100, PVP И F-127) ЗА СОЛАРНЕ ЋЕЛИЈЕ СЕНЗИБИЛИСАНЕ БОЈОМ

JOAN REYES MIRANDA[1,2], ÁNGEL DE JESÚS MORALES RAMÍREZ[1],* FELIPE DE JESÚS CARRILLO ROMO[1], ANTONIETA GARCÍA MURILLO[1], ELDER DE LA ROSA CRUZ3, CÉSAR A. FLORES SANDOVAL[4], ARISTEO GARRIDO HERNÁNDEZ[5] и DULCE YOLOTZIN MEDINA VELÁZQUEZ[2]

[1]Instituto Politécnico Nacional, CIITEC IPN, Cerrada de Cecati S/N. Col. Santa Catarina, Azcapotzalco México D.F. C.P 02250, México, [2]Universidad Autónoma Metropolitana UAM-Azcapotzalco, San Pablo Xalpa No 180. Col Reynosa Tamaulipas, Azcapotzalco, México D.F. C.P. 08100, [3]Centro de Investigaciones en Óptica A.C, A.P. 1-94837150, León, Gto., México, [4]Instituto Mexicano del Petróleo, Programa de Ingeniería Molecular, Eje Central Lázaro Cárdenas No. 152, San Bartolo Atepehuacan, C.P. 07730, Distrito Federal, México и [5]Universidad Tecnológica de Tecámac, División de Nanotecnología, Carretera Federal México-Pachuca Km 37.5, Sierra Hermosa, 55740, Edo. De México, México

Транспарентне TiO_2 фотоелектроде за примену у соларним ћелијама сензибилисаним бојом су синтетисане сол–гел методом и техником потапања. У синтезама су коришћена три реолошка агенса као порозне матрице: Triton X-100, поливинил-пиролидон (M.W. 10000) и Pluronic F-127. У анализи хемијског састава, структуре, морфологије, дебљине и оптичке пропустљивости коришћена је инфрацрвена спектроскопија са Фуријеовом трансформацијом, дифракција X-зрака, скенирајућа електронска микроскопија, спектроскопија m-линије и спектроскопија у видљивој и ултраљубичастој области. Понашање соларне ћелије је испитано спектроскопијом фарадејске импеданције. Просечну ефикасност конверзије енергије од 1,04 % показала је ћелија са фотоелектродом у чијој је синтези коришћењен агенс Triton X-100 као модификатор транспарентности филма TiO_2. У том случају дебљина филма је износила 1,21 μm, димензије кристалита око 7 nm за анатас фазу и порозност 53,4 %. Показано је да је Triton X-100 ефикасан агенс за добијање транспарентних и порозних полупроводних филмова који побољшавају карактеристике фотохемијске ћелије.

(Примљено 15. марта, ревидирано 25. априла, прихваћено 28. априла 2017)

REFERENCES

1. *World Energy Outlook*, International Energy Agency, Paris, 2016
2. M.-H. Sun, S.-Z. Huang, L.-H. Chen, Y. Li, X.-Y. Yang, Z.-Y. Yuan, B.-L. Su, *Chem. Soc. Rev.* **45** (2016) 3479
3. B. O'Regan, M. Gratzel, *Nature* **353** (1991) 737
4. M. Pelaez, N. T. Nolan, S. C. Pillai, M. K. Seery, P. Falaras, A. G. Kontos, P. S. M. Dunlop, J. W. J. Hamilton, J. A. Byrne, K. O'Shea, M. H. Entezari, D. D. Dionysiou, *Appl. Catal., B-Environ.* **125** (2012) 331
5. Y. Wang, Y. He, Q. Lai, M. Fan, *J Environ. Sci.* **26** (2014) 2139
6. Q. Zhou, Z. Fang, J. Li, M. Wang, *Micropor. Mesopor. Mat.* **202** (2015) 22

7. V. Sugathan, E. John, K. Sudhakar, *Renew. Sust. Energ. Rev.* **52** (2015) 54
8. C. Guillén, J. Montero, J. Herrero, *J. Alloys Compd*. **647** (2015) 498
9. Y. Horie, K. Daizaka, H. Mukae, S. Guo, T. Nomiyama, *Electrochim. Acta* **187** (2016) 348
10. Z. Zhao, J. Sun, G. Zhang, L. Bai, *J. Alloys Compd.* **652** (2015) 307
11. L. Avril, S. Bourgeois, P. Simon, B. Domenichini, N. Zanfoni, F. Herbst, L. Imhoff, *Thin.Solid Films, B* **591** (2015) 237
12. J. Du, X. Gu, H. Guo, J. Liu, Q. Wu, J. Zou, *J. Cryst. Growth* **427** (2015) 54
13. M. Fallah, M.-R. Zamani-Meymian, R. Rahimi, M. Rabbani, *Appl. Surf. Sci.* **316** (2014) 456
14. A. Merazga, F. Al-Subai, A. M. Albaradi, A. Badawi, A. Y. Jaber, A. A. B. Alghamdi, *Mat. Sci. Semicon. Proc.* **41** (2016) 114
15. A. C. Pierre, *Introduction to Sol–Gel Processing*, Springer, New York, 1998
16. L. Agartan, D. Kapusuz, J. Park, A. Ozturk, *Ceram. Int.* **41** (2015) 12788
17. E. Blanco, J. M. González-Leal, M. Ramírez-del Solar, *Sol. Energy* **122** (2015) 11
18. M. Z. Yahaya, M. Z. Abdullah, A. A. Mohamad, *J. Alloys Compd.* **651** (2015) 557
19. G. Cao, *Nanostructures & Nanomaterials: Synthesis, Properties & Applications*, Imperial College Press, London, 2004
20. B. Guo, Z. Liu, L. Hong, H. Jiang, *Surf. Coat. Techol*. **198** (2005) 24
21. U. Černigoj, U. L. Štangar, P. Trebše, U. O. Krašovec, S. Gross, *Thin Solid Films* **495** (2006) 327
22. E. C. Muniz, M. S. Góes, J. J. Silva, J. A. Varela, E. Joanni, R. Parra, P. R. Bueno, *Ceram. Int.* **37** (2011) 1017
23. H. Segawa, J. Fukuyoshi, K. Tateishi, K. Tanaka, K. Yoshida, *J. Mater. Sci. Lett.* **22** (2003) 687
24. S. Janitabar-Darzi, A. R. Mahjoub, A. Nilchi, *Physica, E* **42** (2009) 176
25. S. R. Patil, B. H. Hameed, A. S. Škapin, U. L. Štangar, *Chem. Eng. J.* **174** (2011) 190
26. L. Samet, J. Ben Nasseur, R. Chtourou, K. March, O. Stephan, *Mater. Charact.* **85** (2013) 1
27. E. Haimi, H. Lipsonen, J. Larismaa, M. Kapulainen, J. Krzak-Ros, S. P. Hannula, *Thin Solid Films* **519** (2011) 5882
28. S. Doeuff, M. Henry, C. Sanchez, J. Livage, *J. Non-Cryst. Solids* **89** (1987) 206
29. G. Socrates, *Infrared and Raman Characteristics Group Frequencies. Tables and Charts*, John Wiley & Sons, London, 2001
30. D. C. L. Vasconcelos, E. H. M. Nunes, A. C. S. Sabioni, P. M. P. Vasconcelos, W. L. Vasconcelos, *J. Non-Cryst. Solids* **358** (2012) 3042
31. Y.-F. Chen, C.-Y. Lee, M.-Y. Yeng, H.-T. Chiu, *J. Cryst. Growth* **247** (2003) 363
32. G. Kavei, A. Nakaruk, C. Sorrell, *Mater. Sci. Appl.* **2** (2011) 700
33. B. D. Cullity, S. R. Stock, *Elements of X-Ray Diffraction*, Addison-Wesley, Boston, MA, 2001
34. H. Choi, E. Stathatos, D. D. Dionysiou, *Thin Solid Films* **510** (2006) 107
35. O. Šolcova, L. Matejová, P. Kluson, Z. Matej, Z. Strýhal, J. Pavlík, T. Cajthaml, *Sol–Gel Methods for Materials Processing*: *Preparation and Characterization of Thin Nanocrystalline TiO_2 Layers*, Springer, Dordrecht, 2008
36. X. Wang, M. Xi, F. Zheng, B. Ding, H. Fong, Z. Zhu, *Nano Energy* **12** (2015) 794
37. A. Ranjitha, N. Muthukumarasamy, M. Thambidurai, R. Balasundaraprabhu, S. Agilan, *Optik* **124** (2013) 6201
38. D. J. Kim, S. H. Hahn, S. H. Oh, E. J. Kim, *Mater. Lett*. **57** (2002) 355
39. C.-Y. Wu, Y.-L. Lee, Y.-S. Lo, C.-J. Lin, C.-H. Wu, *Appl. Surf. Sci*. **280** (2013) 737

40. M. J. Alam, D. C. Cameron, *J. Sol–Gel Sci. Technol.* **25** (2002) 137
41. L. Skowronski, K. Zdunek, K. Nowakowska-Langier, R. Chodun, M. Trzcinski, M. Kobierski, M. K. Kustra, A. A. Wachowiak, W. Wachowiak, T. Hiller, A. Grabowski, L. Kurpaska, M. K. Naparty, *Surf. Coat. Techol*. **282** (2015) 16
42. J. Tauc, R. Grigorovici, A. Vancu, *Phys. Status Solidi, B* **15** (1966) 627
43. S. Darafarin, R. Sahraei, A. Daneshfar, *J. Alloys Compd*. **658** (2016) 780
44. D. Pjević, T. Marinković, J. Savić, N. Bundaleski, M. Obradović, M. Milosavljević, M. Kulik, *Thin Solid Films, B* **591** (2015) 224
45. J. Tian, H. Deng, L. Sun, H. Kong, P. Yang, J. Chu, *Thin Solid Films* **520** (2012) 5179
46. J. Yang, H. Bai, Q. Jiang, J. Lian, *Thin Solid Films* **516** (2008) 1736
47. S. Valencia, J. M. Marín, G. Restrepo, *Open Mater. Sci. J.* **4** (2010) 9
48. A. Arunachalam, S. Dhanapandian, C. Manoharan, *Physica, E* **76** (2016) 35
49. S. Monneret, P. Huguet-Chantome, F. Flory, *J. Opt., A-Pure Appl. Opt.* **2** (2000) 188
50. R. Ulrich, R. Torge, *Appl. Optics* **12** (1973) 2901
51. M. Buijs, A. Meyerink, G. Blasse, *J. Lumin.* **37** (1987) 9
52. B. E. Yoldas, *Appl. Optics* **19** (1980) 1425
53. M. K. Nazeeruddin, E. Baranoff, M. Grätzel, *Sol. Energy* **85** (2011) 1172
54. M. Gratzel, *Nature* **414** (2001) 338.